

Grounding Object Relations in Language-Conditioned Robotic Manipulation with Semantic-Spatial Reasoning

Qian Luo^{1*}, Yunfei Li^{2*}, Yi Wu^{1,2}

*Indicates equal contribution

¹Shanghai Qi Zhi Institute

²Institute for Interdisciplinary Information Sciences, Tsinghua University
luoqian19961224@gmail.com, liyf20@mails.tsinghua.edu.cn, jxwuyi@gmail.com

Abstract

Grounded understanding of natural language in physical scenes can greatly benefit robots that follow human instructions. In object manipulation scenarios, existing end-to-end models are proficient at understanding semantic concepts, but typically cannot handle complex instructions involving spatial relations among multiple objects, which require both reasoning object-level spatial relations and learning precise pixel-level manipulation affordances. We take an initial step to this challenge with a decoupled two-stage solution. In the first stage, we propose an object-centric semantic-spatial reasoner to select which objects are relevant for the language instructed task. The segmentation of selected objects are then fused as additional input to the affordance learning stage. Simply incorporating the inductive bias of relevant objects to a vision-language affordance learning agent can effectively boost its performance in a custom testbed designed for object manipulation with spatial-related language instructions.

1 Introduction

Understanding complex language instructions is a long-standing research problem for building intelligent robots that can assist humans to perform meaningful tasks in grounded scenes (Chen and Mooney 2011; Bollini et al. 2012; Misra et al. 2016). Recently, there has been exciting progress in grounded vision and language in robotic manipulation scenarios with reinforcement learning and imitation learning (Nair et al. 2021; Jang et al. 2021). Leveraging the power of pretrained vision and language models, some most advanced end-to-end models can effectively ground semantic concepts from natural language to physical scenes and even demonstrate some generalization ability to unseen objects (Shridhar, Manuelli, and Fox 2022a).

However, existing end-to-end agents in vision-language manipulation typically still lack the ability to deal with instructions containing *spatial relations among multiple objects*. Consider a motivating example in Fig. 1 where multiple blocks and bowls with identical or different colors are put on a table. Existing approaches can already follow instructions such as “*put the cyan block into a green bowl*” but cannot handle a more complex instruction like “*place the cyan block in the middle of the front yellow block and*

the back gray bowl”. Solving the previous task only requires understanding simple semantic concepts while the latter one additionally requires the agent to reason over more fine-grained spatial relations.

We hypothesize that current end-to-end models struggle at such complex instructions since it is challenging to simultaneously learn both abstract spatial reasoning and precise manipulation skills in a fully coupled manner. In this paper, we take an initial step towards this challenging problem by decoupling object-level spatial reasoning and pixel-level affordance learning in two stages. We propose an object-centric semantic-spatial reasoning module that predicts which objects are relevant for accomplishing a manipulation task from the language instruction and image observation. Then we fuse the segmentation of all the relevant objects to the input of a strong performing vision-language affordance learning agent CLIPort (Shridhar, Manuelli, and Fox 2022a). The relevant object prediction serves as an effective inductive bias to inform the agent about which regions are beneficial to look at for low-level affordance learning.

To better evaluate whether our proposed framework can effectively handle spatial relations between objects, we design a custom pick-and-place task in cluttered scenes built upon Ravens (Zeng et al. 2021). The language instructions are designed to involve relative spatial positions of objects. Preliminary results show that our method achieves non-trivial success in this task while CLIPort simply cannot work given the same amount of training data.

2 Related Work

Language-conditioned robotic manipulation: Instructing robots with natural language has attracted much research interest in recent years (Mees et al. 2022). Some earlier works proposed end-to-end learning methods for vision-language-conditioned control by imitating large-scale behavior datasets (Lynch and Sermanet 2021; Jang et al. 2021; Mees, Hermann, and Burgard 2022) or learning reward functions for reinforcement learning (Shao et al. 2020; Nair et al. 2021). With advances in multi-modal representation learning (Radford et al. 2021), there are also many works leveraging pretrained vision or language encoders for grounded manipulation tasks (Shridhar, Manuelli, and Fox 2022a,b), and exciting progress in utilizing the planning ability of large language models for embodied reasoning tasks (Ahn et al.

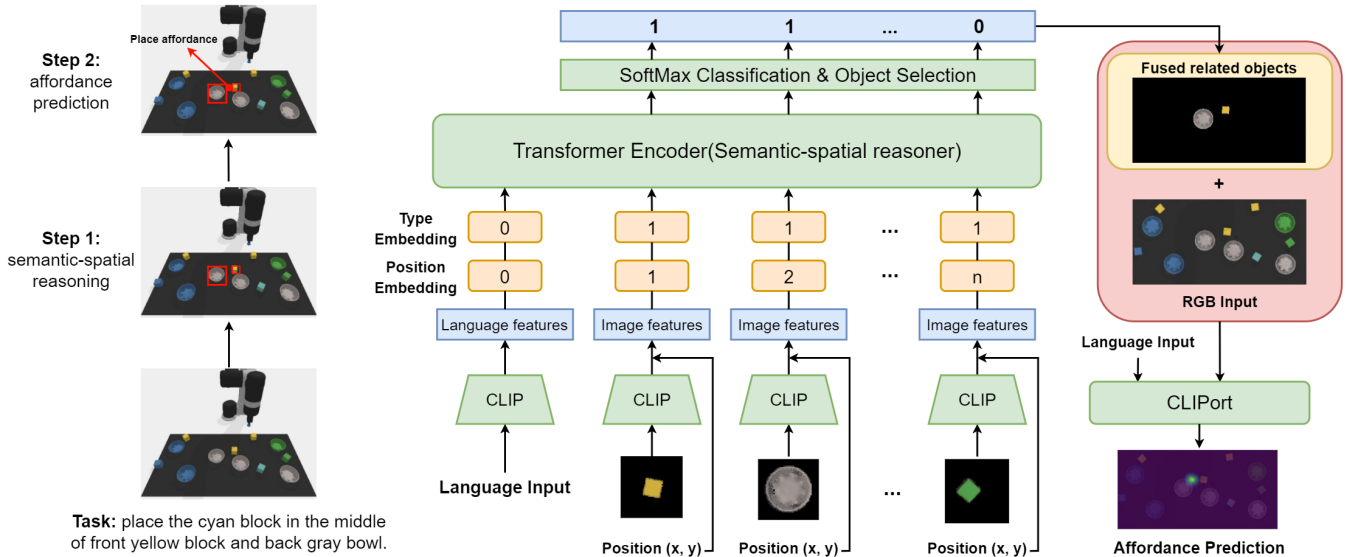


Figure 1: Overview of our two-stage framework for grounding spatial-related instructions in object manipulation tasks.

2022; Zeng et al. 2022; Huang et al. 2022). We are particularly interested in grounding language instructions with complex spatial relations between objects, which cannot be addressed well by previous methods.

Semantic-spatial reasoning for manipulation: Learning spatial relations between different objects have been studied in vision and robotics (Johnson et al. 2017; Mees et al. 2017), which can better address language goals specifying the desired spatial relations (Paul et al. 2016; Venkatesh et al. 2021; Yuan et al. 2021; Liu et al. 2022), and can benefit hierarchical planning to accomplish complex goal configurations (Zhu et al. 2021). A notable line of works study neural-symbolic reasoning to model spatial relations and semantic concepts in a scene (Mao et al. 2019). More recently, fully end-to-end learning mechanism has also achieved much progress in modeling complex object-level relations for visual reasoning with correct inductive bias (Ding et al. 2021). In this work, we also propose a purely data-driven model for semantic-spatial reasoning which is easy to implement and can improve with the increasing scale of the training dataset.

3 Method

We propose a two-stage solution for grounding instructions with spatial relations between objects. In the first stage, a semantic-spatial reasoning module aims to model the object-level relations from language instructions and object-centric image observations (see Sec. 3.1). In the second stage, the segmentation of the selected objects is fed as an additional input to a pixel-level affordance learning model CLIPort, and functions as an inductive bias that guides the agent to attend to particular objects when predicting precise pick and place affordance maps (see Sec. 3.2). Combining with an off-the-shelf object detection and segmentation model, the two stages are cascaded together in deployment (Sec. 3.3).

3.1 Object-centric semantic-spatial reasoning

The semantic-spatial reasoning (SSR) model aims to select relevant objects in a scene for the pick-and-place task given a complex language instruction containing semantic and spatial relations of objects. We leverage a powerful Transformer (Vaswani et al. 2017) architecture to allow grounded understanding of relations from natural language instructions and orthographic RGB images. Specifically, the module takes in an instruction (w_1, w_2, \dots, w_L) , and m image patches with shape $50 \times 50 \times 3$ center-cropped from the detected positions of all the objects along with their (u, v) coordinates in the orthographic image. L is the length of the language instruction and m is the total number of objects in the image. The words and image patches are encoded with the pretrained CLIP model (Radford et al. 2021). The coordinates of objects are encoded with linear layers, then concatenated with the corresponding image patch embeddings into m object-centric features. The L word features and m object-centric features are then concatenated with their position embeddings. To distinguish text and object embeddings, we additionally concatenate type embeddings (0 for texts and 1 for objects) to each token. The $L + m$ tokens are then passed into 8 self-attention layers. The fused features at m object-centric tokens are used to predict scores \hat{s}_i of how related each object is to the language instruction with an MLP. The ground truth for this reasoning module is represented as a binary vector $[s_1, s_2, \dots, s_m]$, where $s_j = 1$ if the j^{th} object is related for performing placement and $s_j = 0$ if the object is irrelevant. Finally, we normalize the scores and the ground truth with softmax and optimize the module to minimize the L_1 distance between them.

Implementations: Our semantic-spatial reasoning module requires cropped object-centric patches as input, which can be predicted from off-the-shelf object detection models. In practice, we adopt an open-vocabulary object detection

model ViLD (Gu et al. 2021) that is suitable for detecting arbitrary categories of objects to predict the locations of all objects. A cheaper way to obtain the image patches when training in simulation is to directly project the center of each object onto the orthographic image, then crop patches with shape $50 \times 50 \times 3$ centered at the projected coordinates.

3.2 Affordance prediction with selected objects

In this part, we describe how we leverage object-level relevance to help low-level manipulation learning.

We adopt a similar two-stream network architecture as CLIPort for predicting pick and place affordance, where a semantic pathway built upon a pretrained CLIP encoder and a spatial pathway based on a transporter network are fused together to predict the pixelwise probability mass $Q_{\text{pick,place}} \in \mathbb{R}^{H \times W}$. For more details, we encourage the readers to refer to the CLIPort paper (Shridhar, Manuelli, and Fox 2022a).

The only difference in our architecture is that our spatial pathway additionally takes as input an attention map indicating which objects may be relevant to the manipulation task. In this way, the affordance prediction model is informed of the high-level semantic-spatial reasoning result and can focus more on the learning of low-level affordance.

The attention map is calculated as follows. After predicting the scores of how relative different objects are to the manipulation task, we select the objects with normalized scores greater than a threshold to guide the affordance prediction stage. We combine the binary segmentation mask of all the selected objects (by computing their logical “OR”) and multiply the mask by the original RGB image to get an attention map with the same shape $(H, W, 3)$ as the original image. The attention map is stacked in channel dimension with the original RGB image as the input to the spatial pathway.

The ground truth of the affordance prediction model is the projected pick and place poses to the 2D image from demonstrations. The training objective is the cross-entropy between normalized $Q_{\text{pick,place}}$ and the ground truth.

3.3 Training and deployment

The semantic-spatial reasoning module and the affordance prediction module are trained separately with supervised learning. We experiment with using oracle object detection and also ViLD detection as input to train the semantic-spatial reasoning module. For affordance prediction module, we always use ground-truth relevant object segmentation as its input during training. In practice, we find our semantic-spatial reasoning module is lightweight for training and can benefit from training over large-scale datasets while training the affordance prediction module is time-consuming and we can only afford training on 1k demos with our best efforts.

During deployment, we first compute the coordinates, cropped patches and segmentation masks of all the objects by querying a ViLD model, then feed the object-centric information along with the language instruction into the semantic-spatial reasoning module to get normalized relevance scores for all the objects. The objects with scores greater than the average are selected and fused into the affordance prediction model to get Q_{pick} and Q_{place} . The best

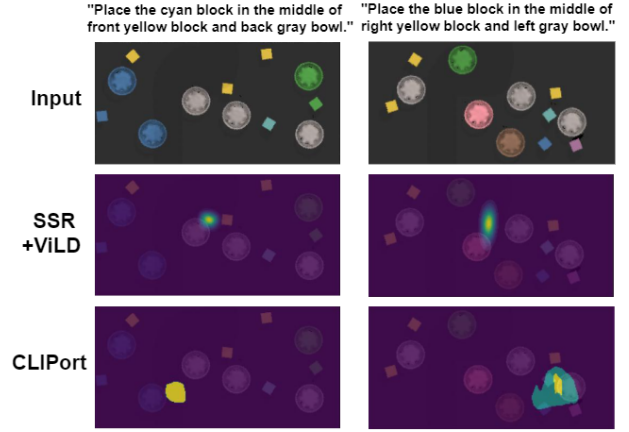


Figure 2: Predicted affordance maps for placement with different methods. Our method can accurately focus on the desired position while CLIPort completely fails.

pick/place location is then computed as $\arg \max_{(u,v)} Q(u, v)$.

Using the parameters of the camera from factory calibration and hand-eye calibration, the 2D locations on the orthographic image can be easily converted to 3D positions relative to the robot base frame. The robot can run any suitable motion planner to reach the desired pick/place poses.

4 Experiments

In this section, we discuss the simulation experiments for validating the proposed method. We design the experiments to answer the following questions.

1. Can our method effectively solve a typical spatial-related pick and place task in Ravens environment?
2. How well does our method perform compared with the baseline method and those validated via ground truth?

4.1 Experimental setup

Task setup We build our task upon Ravens, a collection of simulated tasks in PyBullet (Coumans and Bai 2016–2022) for learning vision-based robotic manipulation. We study a custom language-conditioned pick-and-place task that requires semantic-spatial reasoning. At the beginning of each episode, 6 bowls and 6 blocks are generated at random positions on the table, and objects within each category are of identical shape. Three blocks are of color A, three bowls are of color B and the other six objects are of random colors different from A and B. To test the capability of spatial understanding of our model, the model is supposed to identify the spatial relations among those identical blocks and bowls. The language instructions are generated from the template “pick the [color X] block in the middle of [location a] [color A] block and [location b] [color B] bowl”, in which the locations are sampled from left/right/front/back.

Training details Following the description in the task setup, we generate training, validation and test datasets

Table 1: Pick-and-place success rate of different agents evaluated with seen and unseen objects.

	100 demos		1000 demos		10k demos		100k demos	
	Seen	Unseen	Seen	Unseen	Seen	Unseen	Seen	Unseen
CLIPort	0	0	0	0	N/A	N/A	N/A	N/A
CLIPort oracle	0.45	0.20	0.90	0.59	N/A	N/A	N/A	N/A
SSR + all mask	0.08	0.02	0.36	0.14	0.68	0.34	0.71	0.35
SSR + ViLD	0.02	0.01	0.30	0.11	0.60	0.25	0.65	0.29

in Ravens environment. Specifically, for each sample, the objects are added in accordance with the language instruction described in Sec. 4.1, where `location a` and `location b` are randomly chosen from `left/right/front/back` and `color X`, `color A`, `color B` are randomly selected from a collection of 7 colors. The orthographic RGB image, the cropped oracle object-centric patches together with its projected ground-truth coordinates are added into training instances. The labels include the binary vectors representing the relevance of each object to the given language instruction, and the final pick and place coordinates for grounding.

The training procedures include the semantic-spatial reasoning stage and the affordance prediction stage. In the semantic-spatial reasoning stage, we feed the language instructions, oracle object-centric patches and position information into the transformer, and train the model to fit the normalized binary label. In the affordance prediction stage, we train the downstream CLIPort with segmentation fused from the ground truth of relevant objects.

4.2 Main results

We train each agent with four datasets with different number of demonstrations (100, 1000, 10k, 100k) and choose the best checkpoints on the validation dataset (100 episodes) for evaluation. Each agent is evaluated with the average success rate on the test dataset consisting of 100 cases. An episode is regarded as successful if the correct object is picked and placed within 0.1m distance error to the target position. To test the generalization ability, we evaluate the agents in two settings where the object colors are seen or unseen during training. We compare the performance of four agents:

- **CLIPort:** The agent is trained and evaluated with CLIPort, an end-to-end model that directly predicts pick-and-place affordances from texts and RGBD images.
- **CLIPort with oracle relevant objects:** The agent is trained and evaluated by feeding CLIPort with ground-truth relevant objects. The purpose of this experiment is to verify whether fusing the segmented RGB image of relevant objects to CLIPort can enhance its ability to ground spatial-related language instructions. It approximates the upper bound of the performance if we have a perfect semantic-spatial reasoning module.
- **SSR + all mask:** The agent is trained on SSR module with ground-truth segmentation of all objects. The affordance prediction network is trained separately following the same procedure in **CLIPort with oracle relevant ob-**

jects. The agent is evaluated using ground-truth segmentation of all objects, and the SSR output is fed into the affordance prediction network. The purpose of this experiment is to test the ability of the semantic-spatial reasoning module.

- **SSR + ViLD:** The agent is trained following the same procedure in **SSR + all mask**. The only difference is that we use ViLD segmentation results instead of ground-truth segmentation of all objects. The agent is evaluated in an end-to-end manner without requiring any ground-truth information. The experiment results show how well our model performs without any oracle inputs.

The quantitative experiment results are summarised in Table 1. Since CLIPort already takes 2 days to train with 1000 demos, we cannot afford to train it with 10k and 100k demos. The **CLIPort oracle** agent is also trained on 100/1000 demos, which are used for the affordance prediction of **SSR + all mask** and **SSR + ViLD** agents. We also visualize predicted affordances in Fig. 2.

Our methods (**SSR + ViLD** and **SSR + all mask**) outperform CLIPort in 100 and 1000 demos datasets. With larger datasets, all the agents gain better performance. In all cases, **SSR + all mask** performs slightly better than **SSR + ViLD** agent. The performance gap can be explained by imperfect predictions of ViLD. Our best agent is the **SSR + all mask** agent trained with 100k demos, which reaches a success rate of over 0.7. Since **CLIPort oracle** succeeds in 90 percent of the cases, there is still room to improve for SSR. Our agents are also able to generalize to unseen cases, but the performances are at most 50 percent as good as those in seen cases. We leave a more generalizable agent for future work.

5 Conclusion

In this work, we study the problem of grounded understanding of complex language instructions involving spatial relations between multiple objects in language-conditioned robotic manipulation. We take a preliminary step by enhancing the CLIPort with relevant object masks predicted from an object-centric semantic-spatial reasoning module. Experiment results show that informing the agent of which objects should be focused on is a simple yet effective way to address language-conditioned tasks that require understanding semantic-spatial relations. We plan to extend this work to more general cases with a greater variety of objects and manipulation tasks. Another direction is to work beyond pairwise relations (e.g., left/right) and to tackle multi-object relations (e.g., middle, pyramid).

References

- Ahn, M.; Brohan, A.; Brown, N.; Chebotar, Y.; Cortes, O.; David, B.; Finn, C.; Gopalakrishnan, K.; Hausman, K.; Herzog, A.; Ho, D.; Hsu, J.; Ibarz, J.; Ichter, B.; Irpan, A.; Jang, E.; Ruano, R. J.; Jeffrey, K.; Jesmonth, S.; Joshi, N. J.; Julian, R.; Kalashnikov, D.; Kuang, Y.; Lee, K.; Levine, S.; Lu, Y.; Luu, L.; Parada, C.; Pastor, P.; Quiambao, J.; Rao, K.; Rettinghouse, J.; Reyes, D.; Sermanet, P.; Sievers, N.; Tan, C.; Toshev, A.; Vanhoucke, V.; Xia, F.; Xiao, T.; Xu, P.; Xu, S.; and Yan, M. 2022. Do As I Can, Not As I Say: Grounding Language in Robotic Affordances. *CoRR*, abs/2204.01691.
- Bollini, M.; Tellex, S.; Thompson, T.; Roy, N.; and Rus, D. 2012. Interpreting and Executing Recipes with a Cooking Robot. In Desai, J. P.; Dudek, G.; Khatib, O.; and Kumar, V., eds., *Experimental Robotics - The 13th International Symposium on Experimental Robotics, ISER 2012, June 18-21, 2012, Québec City, Canada*, volume 88 of *Springer Tracts in Advanced Robotics*, 481–495. Springer.
- Chen, D. L.; and Mooney, R. J. 2011. Learning to Interpret Natural Language Navigation Instructions from Observations. In Burgard, W.; and Roth, D., eds., *Proceedings of the Twenty-Fifth AAAI Conference on Artificial Intelligence, AAAI 2011, San Francisco, California, USA, August 7-11, 2011*. AAAI Press.
- Coumans, E.; and Bai, Y. 2016–2022. PyBullet, a Python module for physics simulation for games, robotics and machine learning. <http://pybullet.org>.
- Ding, D.; Hill, F.; Santoro, A.; Reynolds, M.; and Botvinick, M. M. 2021. Attention over Learned Object Embeddings Enables Complex Visual Reasoning. In Ranzato, M.; Beygelzimer, A.; Dauphin, Y. N.; Liang, P.; and Vaughan, J. W., eds., *Advances in Neural Information Processing Systems 34: Annual Conference on Neural Information Processing Systems 2021, NeurIPS 2021, December 6-14, 2021, virtual*, 9112–9124.
- Gu, X.; Lin, T.-Y.; Kuo, W.; and Cui, Y. 2021. Open-vocabulary Object Detection via Vision and Language Knowledge Distillation. In *International Conference on Learning Representations*.
- Huang, W.; Xia, F.; Xiao, T.; Chan, H.; Liang, J.; Florence, P.; Zeng, A.; Tompson, J.; Mordatch, I.; Chebotar, Y.; Sermanet, P.; Brown, N.; Jackson, T.; Luu, L.; Levine, S.; Hausman, K.; and Ichter, B. 2022. Inner Monologue: Embodied Reasoning through Planning with Language Models. *CoRR*, abs/2207.05608.
- Jang, E.; Irpan, A.; Khansari, M.; Kappler, D.; Ebert, F.; Lynch, C.; Levine, S.; and Finn, C. 2021. BC-Z: Zero-Shot Task Generalization with Robotic Imitation Learning. In Faust, A.; Hsu, D.; and Neumann, G., eds., *Conference on Robot Learning, 8-11 November 2021, London, UK*, volume 164 of *Proceedings of Machine Learning Research*, 991–1002. PMLR.
- Johnson, J.; Hariharan, B.; van der Maaten, L.; Fei-Fei, L.; Zitnick, C. L.; and Girshick, R. B. 2017. CLEVR: A Diagnostic Dataset for Compositional Language and Elementary Visual Reasoning. In *2017 IEEE Conference on Computer Vision and Pattern Recognition, CVPR 2017, Honolulu, HI, USA, July 21-26, 2017*, 1988–1997. IEEE Computer Society.
- Liu, W.; Paxton, C.; Hermans, T.; and Fox, D. 2022. StructFormer: Learning Spatial Structure for Language-Guided Semantic Rearrangement of Novel Objects. In *2022 International Conference on Robotics and Automation, ICRA 2022, Philadelphia, PA, USA, May 23-27, 2022*, 6322–6329. IEEE.
- Lynch, C.; and Sermanet, P. 2021. Language Conditioned Imitation Learning Over Unstructured Data. In Shell, D. A.; Toussaint, M.; and Hsieh, M. A., eds., *Robotics: Science and Systems XVII, Virtual Event, July 12-16, 2021*.
- Mao, J.; Gan, C.; Kohli, P.; Tenenbaum, J. B.; and Wu, J. 2019. The Neuro-Symbolic Concept Learner: Interpreting Scenes, Words, and Sentences From Natural Supervision. In *7th International Conference on Learning Representations, ICLR 2019, New Orleans, LA, USA, May 6-9, 2019*. OpenReview.net.
- Mees, O.; Abdo, N.; Mazuran, M.; and Burgard, W. 2017. Metric learning for generalizing spatial relations to new objects. In *2017 IEEE/RSJ International Conference on Intelligent Robots and Systems, IROS 2017, Vancouver, BC, Canada, September 24-28, 2017*, 3175–3182. IEEE.
- Mees, O.; Hermann, L.; and Burgard, W. 2022. What Matters in Language Conditioned Robotic Imitation Learning Over Unstructured Data. *IEEE Robotics and Automation Letters*, 7(4): 11205–11212.
- Mees, O.; Hermann, L.; Rosete-Beas, E.; and Burgard, W. 2022. CALVIN: A Benchmark for Language-Conditioned Policy Learning for Long-Horizon Robot Manipulation Tasks. *IEEE Robotics Autom. Lett.*, 7(3): 7327–7334.
- Misra, D. K.; Sung, J.; Lee, K.; and Saxena, A. 2016. Tell me Dave: Context-sensitive grounding of natural language to manipulation instructions. *Int. J. Robotics Res.*, 35(1-3): 281–300.
- Nair, S.; Mitchell, E.; Chen, K.; Ichter, B.; Savarese, S.; and Finn, C. 2021. Learning Language-Conditioned Robot Behavior from Offline Data and Crowd-Sourced Annotation. In Faust, A.; Hsu, D.; and Neumann, G., eds., *Conference on Robot Learning, 8-11 November 2021, London, UK*, volume 164 of *Proceedings of Machine Learning Research*, 1303–1315. PMLR.
- Paul, R.; Arkin, J.; Roy, N.; and Howard, T. M. 2016. Efficient Grounding of Abstract Spatial Concepts for Natural Language Interaction with Robot Manipulators. In Hsu, D.; Amato, N. M.; Berman, S.; and Jacobs, S. A., eds., *Robotics: Science and Systems XII, University of Michigan, Ann Arbor, Michigan, USA, June 18 - June 22, 2016*.
- Radford, A.; Kim, J. W.; Hallacy, C.; Ramesh, A.; Goh, G.; Agarwal, S.; Sastry, G.; Askell, A.; Mishkin, P.; Clark, J.; et al. 2021. Learning transferable visual models from natural language supervision. In *International Conference on Machine Learning*, 8748–8763. PMLR.
- Shao, L.; Migimatsu, T.; Zhang, Q.; Yang, K.; and Bohg, J. 2020. Concept2Robot: Learning Manipulation Concepts from Instructions and Human Demonstrations. In Toussaint, M.; Biechi, A.; and Hermans, T., eds., *Robotics: Science and*

Systems XVI, Virtual Event / Corvallis, Oregon, USA, July 12-16, 2020.

Shridhar, M.; Manuelli, L.; and Fox, D. 2022a. Cliport: What and where pathways for robotic manipulation. In *Conference on Robot Learning*, 894–906. PMLR.

Shridhar, M.; Manuelli, L.; and Fox, D. 2022b. Perceiver-Actor: A Multi-Task Transformer for Robotic Manipulation. *CoRR*, abs/2209.05451.

Vaswani, A.; Shazeer, N.; Parmar, N.; Uszkoreit, J.; Jones, L.; Gomez, A. N.; Kaiser, Ł.; and Polosukhin, I. 2017. Attention is all you need. *Advances in neural information processing systems*, 30.

Venkatesh, S. G.; Biswas, A.; Upadrashta, R.; Srinivasan, V.; Talukdar, P.; and Amrutur, B. 2021. Spatial Reasoning from Natural Language Instructions for Robot Manipulation. In *IEEE International Conference on Robotics and Automation, ICRA 2021, Xi'an, China, May 30 - June 5, 2021*, 11196–11202. IEEE.

Yuan, W.; Paxton, C.; Desingh, K.; and Fox, D. 2021. SOR-Net: Spatial Object-Centric Representations for Sequential Manipulation. In Faust, A.; Hsu, D.; and Neumann, G., eds., *Conference on Robot Learning, 8-11 November 2021, London, UK*, volume 164 of *Proceedings of Machine Learning Research*, 148–157. PMLR.

Zeng, A.; Florence, P.; Tompson, J.; Welker, S.; Chien, J.; Attarian, M.; Armstrong, T.; Krasin, I.; Duong, D.; Sindhwani, V.; et al. 2021. Transporter networks: Rearranging the visual world for robotic manipulation. In *Conference on Robot Learning*, 726–747. PMLR.

Zeng, A.; Wong, A.; Welker, S.; Choromanski, K.; Tombari, F.; Purohit, A.; Ryoo, M. S.; Sindhwani, V.; Lee, J.; Vanhoucke, V.; and Florence, P. 2022. Socratic Models: Composing Zero-Shot Multimodal Reasoning with Language. *CoRR*, abs/2204.00598.

Zhu, Y.; Tremblay, J.; Birchfield, S.; and Zhu, Y. 2021. Hierarchical Planning for Long-Horizon Manipulation with Geometric and Symbolic Scene Graphs. In *IEEE International Conference on Robotics and Automation, ICRA 2021, Xi'an, China, May 30 - June 5, 2021*, 6541–6548. IEEE.